ELSEVIER

Catalysis Today 23 (1995) 403–408

CATALYSIS TODAY

Density functional calculations on agostic ethyl–Ti(IV) complexes

Hiroaki Munakata[a,b,*], Yukiko Ebisawa[b], Yuka Takashima[b], Michael C. Wrinn[c], Andrew C. Scheiner[c], John M. Newsam[c]

[a]*Research Institute of Innovative Technology for the Earth, 9-2, Kizugawadai, Kizu-cho, Sorakugun, Kyoto 619-02, Japan*
[b]*Ryoka Systems Inc., 1-5-2, Irifune, Urayasu City, Chiba 279, Japan*
[c]*Biosym Technologies Inc., 9685 Scranton Road, San Diego, CA 92121-2777, USA*

Abstract

First principles, density functional theory embodied in the DMol program has been applied to agostic ethyl–Ti-complexes, including the dmpe complex, $[Ti(-CH_2CH_3)Cl_3(dmpe)]$, where dmpe = $(Me_2PCH_2)_2$ and its model complex, $[Ti(-CH_2CH_3)Cl_3(PH_3)_2]$. The ethyl moiety of the complexes can adopt two limiting conformations, staggered and eclipsed. In the model complex, $[Ti(-CH_2CH_3)Cl_3(PH_3)_2]$, both conformers are found to form agostic structures upon geometry optimization subject to Cs symmetry constraint, with the agostic eclipsed structure being the lower in energy. Full geometry optimization of the dmpe complex, $[Ti(-CH_2CH_3)Cl_3(dmpe)]$, yields an agostic structure with geometrical features similar to those measured by single crystal X-ray analysis. It is shown that the HOMO orbital contributes substantially to the agostic bonding.

1. Introduction

A metal-bonded alkyl carbon–hydrogen bond can interact as a ligand with an electronically unsaturated transition metal center. This interaction is known as an agostic interaction. Agostic organometallic complexes play an important role in catalytic Ziegler–Natta polymerization and in metal bonded alkyl β–C–H hydrogen elimination. The exemplary agostic compounds, $[Ti(-R)Cl_3(dmpe)]$, (R = Me or Et; dmpe = $Me_2PCH_2CH_2PMe_2$) were prepared and their structures were characterized by X-ray and neutron diffraction. The compound (R = Et) exhibited an agostic interaction between the metal bonded ethyl β-C–H and the central Ti atom [1,2]. Koga and Morokuma [3] performed theoretical calculations on the model compound $[Ti(-CH_2CH_3)Cl_2H(PH_3)_2]$, derived from the original compound, $[Ti(-CH_2CH_3)Cl_3(dmpe)]$, by replacing dmpe by two PH_3 groups and one of the three chlorine ligands, trans to the phosphorous atom of dmpe, by hydrogen. The calculations at the Hartree–Fock (HF) level produced the agostic structure upon geometry optimization.

Recently, it has been shown that density functional theory (DFT) method provides accurate results for the geometries and other properties for transition metal compounds [4,5]. The DFT method is suited for large molecular systems, as the time required by DFT methods in the local density approximation (LDA) scales formally as only N^3 (N = number of electrons in the system).

*Corresponding author.

SSDI 0920-5861(94)00156-1

The present study applies DFT, as embodied efficiently in the DMol code [6,7], to the model compound, $[Ti(-CH_2CH_3)Cl_3(PH_3)_2]$ and to the original compound, $[Ti(-CH_2CH_3)Cl_3(dmpe)]$. We consider the applicability to large molecular systems and examine the geometries, energetics and agostic interactions in these organotitanium complexes.

2. Method and DFT calculation details

Molecular electronic energies and energy gradients were computed mostly at the local density functional (LDF) level of theory with DMol [8] using the Hedin–Lundqvist/Janak–Morruzi–Williams local correction functionals (JMW) [9] or the VWN local correction functionals derived in the Vosko–Wilk–Nusair parameterization of Ceperley and Alder's electron gas Monte Carlo data [10,11]. The atomic orbital basis set used throughout was the standard DMol double numerical + polarization (DNP) basis obtained from exact numerical LDF calculations on the constituent atoms and cationic states of these same atoms. Additionally, only the molecular orbital (MO) coefficients corresponding to valence orbitals were included in the self-consistent field (SCF) procedure. Thus the MO coefficients corresponding to the Ti core 1s2s2p, the P and Cl 1s2s, and the C 1s orbitals were fixed at their atomic values in the molecular SCF procedure.

In order to facilitate the DFT calculations, a simplified model, $[Ti(-CH_2CH_3)Cl_3(PH_3)_2]$, of

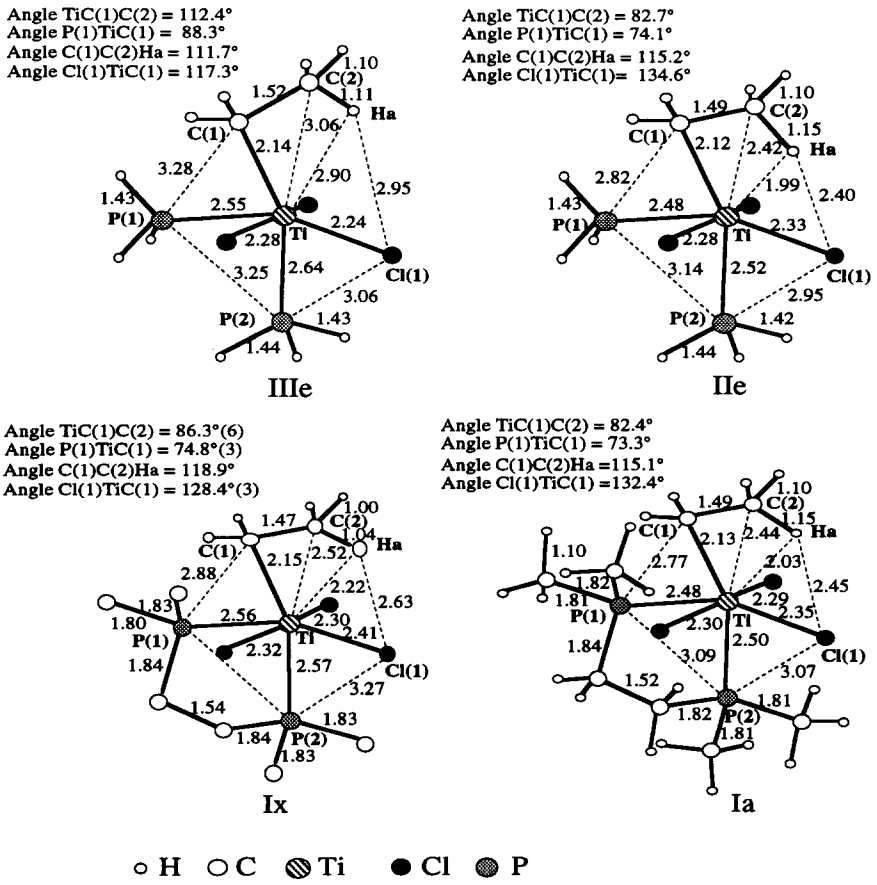

Fig. 1. Structures of non-agostic and agostic Ti complexes: (IIIe) non-agostic model structure with an eclipsed ethyl ligand, (IIe) agostic model structure with an eclipsed ethyl ligand, (Ix) X-ray crystallographic structure of the agostic Ti complex, (Ia) LDF optimized structure of the Ti complex (Ix).

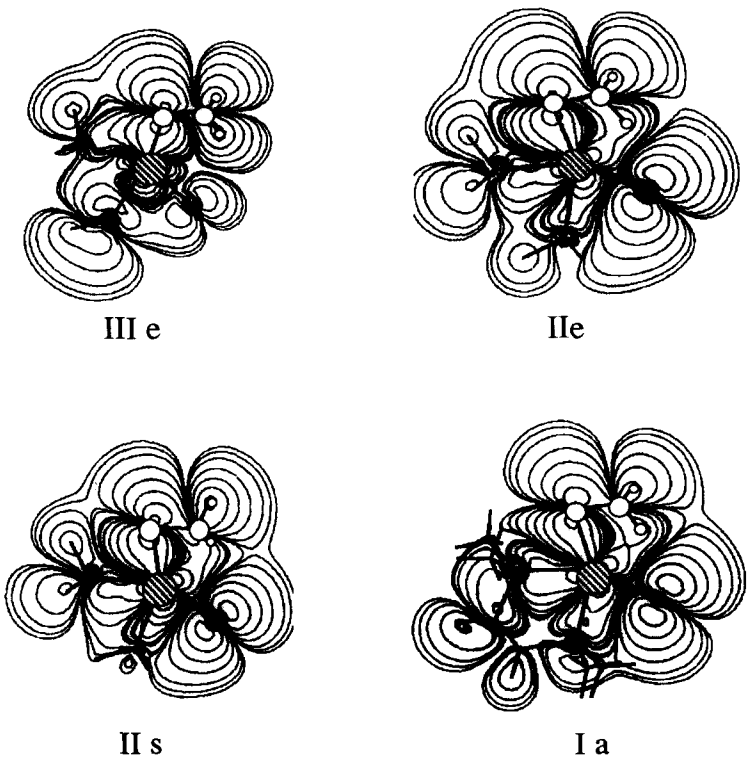

Fig. 2. HOMO contour maps of LDF optimized structures: non-agostic model with an eclipsed ethyl ligand (IIIe), corresponding agostic model structure with an eclipsed ethyl ligand (IIe), corresponding agostic model structure with a staggered ethyl ligand (IIs), and LDF optimized structure of $Ti(-CH_2CH_3)Cl_3(dmpe)$ (Ia).

the complex $[Ti(-CH_2CH_3)Cl_2(dmpe)]$ (Ix) characterized structurally by X-ray diffraction was derived by replacing the dmpe ligand with two PH_3 groups. Two conformers of the model compound, $[Ti(-CH_2CH_3)Cl_3(PH_3)_2]$ were studied, corresponding to eclipsed and staggered conformations of the ethyl ligand.

The LDF geometry optimizations of the two conformers subject to the constraints of Cs symmetry led to agostic structures, both for the eclipsed ethyl ligand Ti complex structure (IIe), and for the staggered configuration (IIs).

To explore the energy differences between agostic and non-agostic structures, non-agostic configurations of the eclipsed and staggered ethyl ligands were derived as follows.

To configure a non-agostic model complex with the eclipsed ethyl ligand, the ethyl ligand of the DMol optimized agostic model complex with the eclipsed ethyl structure was distorted into a normal ethyl configuration with a C(2)–C(1)–Ti bond angle of 112.4°, a H_a–C(2)–C(1) bond angle of 111.7°, and a C(1)–C(2) bond distance of 1.52 Å. Such geometrical parameters were derived from the eclipsed ethyl part of DMol-optimized propane with an eclipsed configuration. The C(1)–Ti bond distance of the complex was set to 2.14 Å. An LDF geometry optimization of this normal ethyl ligand structure was then carried out but subject to a geometrical constraint on atoms, C(1), C(2), H_a, and Ti, by fixing cartesian coordinates of these atoms. The optimized non-agostic eclipsed ethyl ligand structure (IIIe) was thus obtained.

The non-agostic staggered ethyl ligand structure (IIIs) was produced by rotating the methyl group of the optimized eclipsed conformer by 180°. The LDF energy calculation was then carried out on this structure without geometry relaxation.

The geometries of the non-agostic (IIIe) and agostic (IIe) complex configurations for the eclipsed ethyl ligand conformation are shown in Fig. 1.

Contour maps of the highest occupied molecular orbitals (HOMO) obtained for the LDF calculated structures [(Ia), (IIe), (IIs) and (IIIe)] are given in Fig. 2.

The initial dmpe complex structure, $[Ti(-CH_2CH_3)Cl_3(dmpe)]$, for the LDF calculation was derived from the X-ray analyzed structure by adding the necessary missing hydrogens. The LDF optimization of the dmpe complex, $[Ti(-CH_2CH_3)Cl_3(dmpe)]$, was successfully achieved, although convergence was complicated by the size of this molecule, 35 atoms.

The optimized dmpe complex structure (Ia) is given in Fig. 1 together with the original dmpe complex structure (Ix) characterized by X-ray diffraction.

Recently the DFT method has been advanced by introducing non-local corrections. DMol has been enhanced by the implementation of Becke's 1988 version of a gradient corrected functional (B88) [12] and the Lee–Yang–Parr (1988) correlation functional (LYP) [13].

As part of this study we have applied this new methodology to the present agostic ethyl Ti (IV) complexes.

A non-local DFT geometry optimization with the B88 and Lee–Yang–Parr functionals was performed on the agostic model structure with the eclipsed ethyl ligand conformation (IIe). The non-local DFT optimized structure (IVe) is shown in Fig. 3. InsightII [14] and the modules developed by Catalysis & Sorption Project [15] were used for the graphics display and analysis.

3. Discussion

The relative binding energy relationships at the local DFT level for agostic and non-agostic configurations of the eclipsed and the staggered ethyl ligand conformation are shown in Fig. 4. The eclipsed ethyl ligand conformer (IIe) was found

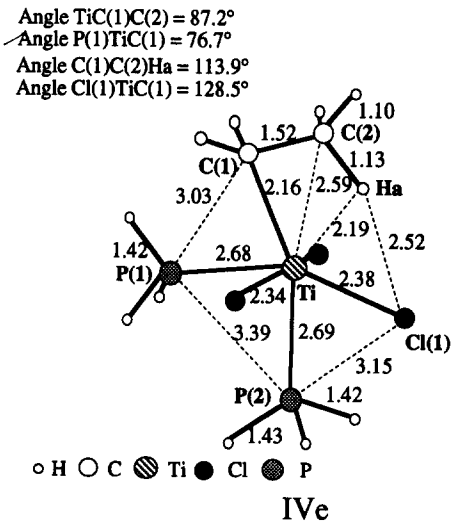

Fig. 3. Geometry of the agostic model complex structure as optimized by non-local DFT.

to have a lower energy than the staggered conformer (IIs) in the agostic configuration, whereas the staggered ethyl ligand structure (IIIs) was found to be lower in energy than the eclipsed structure (IIIe) in the non-agostic configuration.

The binding energy differences between agostic and non-agostic structures were calculated to be 12.4 kcal/mol for the eclipsed conformation and 8.6 kcal/mol for the staggered conformation and

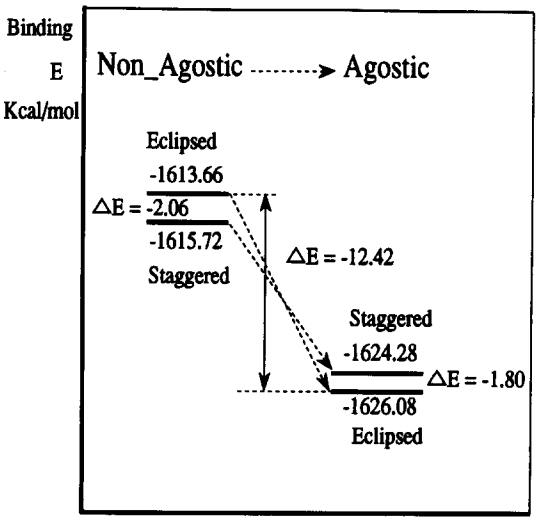

Fig. 4. Binding energy relationships at the local DFT level for the non-agostic and agostic configuration of the eclipsed and staggered ethyl ligand conformation.

both the eclipsed and staggered conformers were stabilized in the agostic state.

The geometry data of the optimised agostic structures are compared with the experimental data of the X-ray analysed structure (Ix) and given in Table 1.

The LDF optimized structure of the dmpe complex (Ia) is in reasonable agreement with the X-ray structural data; the RMS deviation for the atom-atom distances in Table 1 is 0.109. Larger deviations are observed for distances between the hydrogen and the heavy atoms. The hydrogen atom positions determined by X-ray analysis are likely to be relatively imprecise.

LDF geometry optimizations without non-local corrections tend to give slightly shorter bond lengths and this tendency is also observed in this case.

With respect to the bond angles, the optimized structure of the dmpe complex (Ia) showed Ti–C(1)–C(2) bond angle of 82.4° (compared with the experimental, Ix, 86.3°), a C1–C2–H_a bond angle of 115.1° (Ix, 118.9°) and a P(1)–Ti–C(1) bond angle of 73.3° (Ix, 74.8°). This set of angles characterizes the agostic structure.

The Local DFT optimised structure (IIe) for the simplified model compound with the eclipsed ethyl ligand conformation also showed good agreement with the experimental structure. The RMS deviation for the atom–atom distances in Table 1 is 0.139. The larger deviations are observed again for distances involving hydrogen.

The optimized model structure (IIe) showed a Ti–C(1)–C(2) bond angle of 82.7° (compared with the experimental value for the dmpe complex, Ix, 86.3°), a C(1)–C(2)–H_a bond angle of 115.2° (Ix, 118.9°) and a P(1)–Ti–C(1) bond angle of 74.1° (Ix, 74.8°). The LDF optimised agostic structure of the model compound (IIe) shows bond distances and bond angles close to those in the LDF optimized structure (Ia) of the dmpe complex.

The structure (IVe) of the simplified model compound with the eclipsed ethyl ligand optimized at the non-local level showed a smaller RMS deviation, 0.087, for the atom–atom dis-

Table 1
Comparison of the geometric data for optimized agostic structures

Inter-atom distances (Å) and angles (°)	Exp. X-ray dmpe complex Ix	DMol (local) dmpe complex		DMol (local) model		DMol (non-local) model	
		Ia	Δ	IIe	Δ	IVe	Δ
Ti–Cl(1)	2.408(3)	2.35	−0.06	2.33	−0.08	2.38	−0.03
Ti–Cl(2)	2.323(3)	2.30	−0.02	2.28	−0.04	2.34	+0.02
Ti–Cl(3)	2.303(3)	2.29	−0.01	2.28	−0.02	2.34	+0.04
Ti–P(1)	2.560(3)	2.48	−0.08	2.48	−0.08	2.68	+0.12
Ti–P(2)	2.570(3)	2.50	−0.07	2.52	−0.05	2.69	+0.12
Ti–C(1)	2.151(9)	2.13	−0.02	2.12	−0.03	2.16	+0.01
Ti–C(2)	2.524(10)	2.44	−0.08	2.42	−0.10	2.59	+0.07
Ti–H_a	2.22(10)	2.03	−0.19	1.99	−0.23	2.19	−0.03
C(1)–C(2)	1.467(15)	1.49	+0.02	1.49	+0.02	1.52	+0.05
C(2)–H_a	1.04(2)	1.15	+0.11	1.15	+0.11	1.13	+0.09
Cl(1)–H_a	2.63	2.45	−0.18	2.40	−0.23	2.52	−0.11
C(1)–P(1)	2.88	2.77	−0.11	2.82	−0.06	3.03	+0.15
Cl(1)–P(2)	3.27	3.07	−0.20	2.95	−0.32	3.15	−0.12
RMS			0.109		0.139		0.087
Ti–C(1)–C(2)	86.3(6)	82.4	−3.9	82.7	−3.6	87.2	+0.9
C(1)–C(2)–H_a	118.9	115.1	−3.8	115.2	−3.7	113.9	−5.0
P(1)–Ti–C(1)	74.8(3)	73.3	−1.5	74.1	−0.7	76.7	+1.9
P(1)–Ti–P(2)	74.75(9)	76.1	+1.3	77.2	+2.5	78.3	+3.6
Cl(1)–Ti–P(2)	82.1(1)	78.4	−3.7	74.1	−8.0	76.6	−5.5
Cl(1)–Ti–C(1)	128.4(3)	132.4	+4.0	134.6	+6.2	128.5	+0.1

tances in Table 1. Several of the atom–atom distances that were short at the local level are now longer. Larger deviations occure in the Ti–P(1) and Ti–P(2) bond distances. This suggests that the larger deviation in the Ti–P(1) and Ti–P(2) bond distances for the non-local DFT optimized structure (IVe) was due to replacing the dmpe ligand by two phosphine ligands. The optimized structure (IVe) has a Ti–C(1)–C(2) bond angle of 87.2°, very close to experimental value for the dmpe complex (Ix, 86.3°), a C(1)–C(2)–H_a bond angle of 113.9° (Ix, 118.9°) and a P(1)–Ti–C(1) bond angle of 76.7° (Ix, 74.8°).

In all of the agostic structures examined in this study, the highest occupied molecular orbital (HOMO), which mainly involves the Ti $3d_{xy}$ and H_a 1s atomic orbitals contributed principally to the agostic bonding.

4. Conclusion

Geometry optimizations by the DFT method implemented in DMol reproduced the agostic structures for both the dmpe complex characterized structurally by X-ray diffraction and the simplified model complex in which the dmpe ligand was replaced by two PH_3 ligands. The computational cost is substantially reduced when using the simpler model ligands and symmetry constraints.

The relative binding energy difference between agostic and non-agostic structures at the LDF level was estimated to be 9–12 kcal/mol for the simplified model complex. Both eclipsed and staggered conformations of the ethyl ligand in the Ti(IV) complexes converged to agostic structures on DMol geometry optimization.

Use of non-local corrections to the DFT method improved the optimized geometry of the agostic model compound, and the agostic configuration of the ethyl ligand was in good agreement with the X-ray structure analysis results, for the Ti–C(1)–C(2) angle of 87.2°, compared with the experimental value of 86.3°.

In all of the agostic structures studied, the highest occupied molecular orbitals contributed substantially to the agostic bonding, involving Ti–$3d_{xy}$ and H_a 1s atomic orbitals.

Acknowledgment

This research was supported in part by the NEDO Environmental Catalyst Research Project. This research was also supported in part by Ryoka Systems Inc. The BIOSYM Catalysis and Sorption project is supported by a consortium of industrial, government and academic institutions.

References

[1] Z. Dawoodi, M.L.H. Green, V.S.B. Mtewa, C.K. Prout, A.J. Schults, J.M. Williams and T.F. Koetzle, J. Chem. Soc., Dalton Trans., (1986) 1629–1637.
[2] M. Brookhart and M.L. Green, J. Organomet. Chem., 250 (1983) 395–408.
[3] N. Koga and K. Morokuma, J. Am. Chem. Soc., 106 (1984) 4625–4626.
[4] C. Sosa, J. Andzelm, B.C. Elkin, E. Wimmer, K.D. Dobbs and D. Dixon, J. Phys.Chem., 96 (1992) 6630–6636.
[5] E. Folga and T. Ziegler, J. Am. Chem. Soc., 115 (1993) 5169–5176.
[6] B. Delley, J. Chem. Phys., 92 (1990) 508.
[7] B. Delley, J. Chem. Phys., 94 (1991) 7245.
[8] DMol, version 2.2.0, Biosym Technologies, San Diego, (1992); Version 2.3.0 (1993).
[9] L. Hedin and B.I. Lundqvist, J. Phys. Chem., 4 (1971) 2064.
[10] S.J. Vosko, L. Wilk and M. Nuair, Can. J. Phys., 58 (1980) 1200–1211.
[11] D.M. Ceperley and B.J. Alder, Phys. Rev. Lett., 45 (1980) 566–569.
[12] A.D. Becke, J. Chem. Phys., 88 (1988) 2547.
[13] C. Lee, W. Yang and R.G. Parr, Phys. Rev. B, 37 (1988) 786.
[14] InsightII, version 2.3.0, Biosym Technologies, San Diego (1993).
[15] Catalysis and Sorption Project Modules, version 4.0, Biosym Technologies, San Diego (1993).